

Orbital selective correlations between nesting/scattering/Lifshitz transition and the superconductivity in $\text{AFe}_{1-x}\text{Co}_x\text{As}$ ($\text{A}=\text{Li}, \text{Na}$)

Z. R. Ye,¹ Y. Zhang,¹ M. Xu,¹ Q. Q. Ge,¹ Q. Fan,¹ F. Chen,¹ J. Jiang,¹ P. S. Wang,² J. Dai,² W. Yu,² B. P. Xie,^{1,*} and D. L. Feng^{1,†}

¹State Key Laboratory of Surface Physics, Department of Physics,
and Advanced Materials Laboratory, Fudan University, Shanghai 200433, People's Republic of China

²Department of Physics, Renmin University of China, Beijing 100872, China

(Dated: June 13, 2018)

The correlations between the superconductivity in iron pnictides and their electronic structures are elusive and controversial so far. Here through angle-resolved photoemission spectroscopy measurements, we show that such correlations are rather distinct in $\text{AFe}_{1-x}\text{Co}_x\text{As}$ ($\text{A}=\text{Li}, \text{Na}$), but only after one realizes that they are orbital selective. We found that the superconductivity is enhanced by the Fermi surface nesting, but only when it is between d_{xz}/d_{yz} Fermi surfaces, while for the d_{xy} orbital, even nearly perfect Fermi surface nesting could not induce superconductivity. Moreover, the superconductivity is completely suppressed just when the d_{xz}/d_{yz} hole pockets sink below Fermi energy and evolve into an electron pocket. Our results thus establish the orbital selective relation between the Fermiology and the superconductivity in iron-based superconductors, and substantiate the critical role of the d_{xz}/d_{yz} orbitals. Furthermore, around the zone center, we found that the d_{xz}/d_{yz} -based bands are much less sensitive to impurity scattering than the d_{xy} -based band, which explains the robust superconductivity against heavy doping in iron-based superconductors.

PACS numbers: 74.25.Jb, 74.70.-b, 79.60.-i, 71.20.-b

The orbital degree of freedom is responsible for many emergent properties in correlated materials. For example in transition-metal oxides, due to the multiplicity of orbitals, the system often exhibits complex orbital and charge orderings [1]. In manganese oxides, t_{2g} orbitals are strongly localized, while e_g orbitals are itinerant. Such different characters of different orbitals and the Hund's coupling among them lead to the colossal magnetoresistance effect [2]. In the iron-based high temperature superconductors (Fe-HTS's), the orbital degree of freedom also plays an important role. In the parent compounds, a nematic electronic state has been discovered prior to the magnetic order, indicating the existence of orbital ordering and orbital fluctuations [3–5]. In the superconducting state, the gap anisotropy, nodes, and multi-gap behaviors have been observed [6, 7], which might be attributed to the different orbital compositions of the Fermi surfaces (FSs).

Certain orbital dependencies of various properties in iron pnictides are expected as for any multi-orbital system, however so far, the distinctive roles played by various orbitals remain unclear. Models including three, five or even more orbitals have been proposed to make quantitative calculations and comparisons [8, 9], however, they practically conceal the dominating physics with complexity as well. In search of the critical correlations between superconductivity and electronic structures, at first, the nesting between any hole FS at the zone center and any electron FS at the zone corner was suggested to be important for the superconductivity, without distinguishing the orbital characters [10–12]. Later on, it was pointed out in $\text{BaFe}_{2-x}\text{Co}_x\text{As}_2$ [13] and LiFeAs [14] that FS nesting is unnecessary, while the presence of central hole pockets or Van Hove singularity are more important. Again, the orbital degree of freedom was ignored in these studies, and the several hole pockets originated from different orbitals in $\text{BaFe}_{2-x}\text{Co}_x\text{As}_2$ were not resolved. On

the other hand, the majority of theoretical studies indicate that the inter-pocket nesting would significantly enhance the superconductivity [15, 16]. Therefore, these contradicting correlations between the Fermi surface topology (or Fermiology for short) and the superconductivity create confusion, since they are all partially supported by different experiments and theories. It hampers a clear picture as to what determines the superconductivity in Fe-HTS's.

In this Letter, we examine the roles of different orbitals in the superconductivity of Fe-HTS's with angle resolved photoemission spectroscopy (ARPES) studies on $\text{LiFe}_{1-x}\text{Co}_x\text{As}$ and $\text{NaFe}_{1-x}\text{Co}_x\text{As}$. With unpolar surface, and simple orbital characters of various FSs, these two systems are ideal for studying the orbital-selective role of the Fermiology in the superconductivity. We found the FS nesting effect on superconductivity is orbital selective; even perfect nesting for the d_{xy} Fermi pockets in $\text{LiFe}_{0.83}\text{Co}_{0.17}\text{As}$ could not induce superconductivity, while the perfect nesting between d_{xz}/d_{yz} Fermi pockets corresponds to the maximal superconducting transition temperature (T_C) in $\text{NaFe}_{1-x}\text{Co}_x\text{As}$. In addition, we found that superconductivity is completely suppressed when the d_{xz}/d_{yz} hole pockets evolve into an electron pocket (a Lifshitz transition). Furthermore, around the zone center, we observed that the d_{xy} -based band is much more susceptible to impurity scattering than the d_{xz}/d_{yz} -based bands. Our results give a distinct description of the roles of different orbitals, and establish a pivotal correlation between Fermiology and superconductivity, which could resolve the previous controversies and simplify theories on the superconductivity.

High quality $\text{AFe}_{1-x}\text{Co}_x\text{As}$ ($\text{A}=\text{Li}, \text{Na}$) single crystals of various dopings were synthesized with self-flux method (See supplementary material), covering a large portion of the phase diagrams [Figs. 1(a) and 1(b)]. For $\text{LiFe}_{1-x}\text{Co}_x\text{As}$, superconductivity was observed in $x=0, 0.03$, and 0.09 samples (named

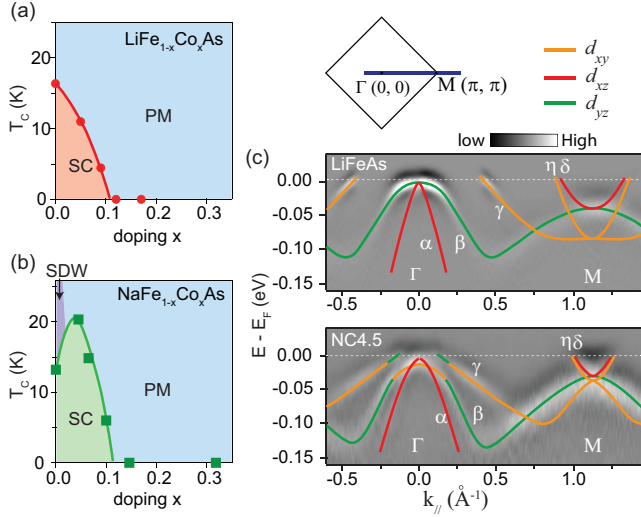


FIG. 1: (a) and (b), The phase diagrams of $\text{LiFe}_{1-x}\text{Co}_x\text{As}$ and $\text{NaFe}_{1-x}\text{Co}_x\text{As}$, respectively. Transport measurements could be found in the supplementary information. (c) The second derivative photoemission spectra taken in LiFeAs and NC4.5 along the Γ -M direction. The orbital distribution and band structure are overlaid on the spectra. The same color code for different orbitals is used throughout this paper.

as LiFeAs , LC3 , and LC9 hereafter by their dopant percentages) with T_c of 16.4, 11, and 4.4 K, respectively [Fig. 1(a)]. For $\text{NaFe}_{1-x}\text{Co}_x\text{As}$, the T_c 's are 13, 20.3, 14.8, and 6 K for $x=0, 0.045, 0.065$, and 0.1 respectively (named as NaFeAs , NC4.5 , NC6.5 , and NC10 hereafter) [Fig. 1(b)]. ARPES measurements were performed at Fudan University with a 7 eV Laser or 21.2 eV light from a helium discharging lamp, and also at various beamlines, including the beamline 5-4 of Stanford Synchrotron Radiation Lightsources (SSRL), the beamline 9A of Hiroshima Synchrotron Radiation Center (HiSOR) and the SIS beamline of Swiss Light Source (SLS). All the data were taken with Scienta R4000 electron analyzers. The overall energy resolution was 5~10 meV at Fudan, SSRL and HiSOR, or 15~20 meV at SLS depending on the photon energy, and the angular resolution was 0.3 degree. The samples were cleaved *in situ*, and measured in ultrahigh vacuum with pressure better than 3×10^{-11} torr.

The orbital characters and band structures of LiFeAs and NaFeAs have been well studied by previous ARPES measurements [14, 17, 18]. There are three hole bands near Γ and two electron bands near M . We compare the spectra taken along Γ -M direction for LiFeAs and NC4.5 as shown in Fig. 1(c). The band structures are very similar except for the d_{xy} band. In LiFeAs , the γ band with the d_{xy} orbital crosses the Fermi energy (E_F) around the zone center forming a large hole pocket. However, in NC4.5 , the d_{xy} band disperses well below E_F and hybridizes with the d_{yz} band. Therefore, the d_{xy} orbital does not contribute to the FS. Intriguingly, T_c is almost the same for LiFeAs and NC4.5 , no matter whether the d_{xy} orbital is present on the zone center FS or not.

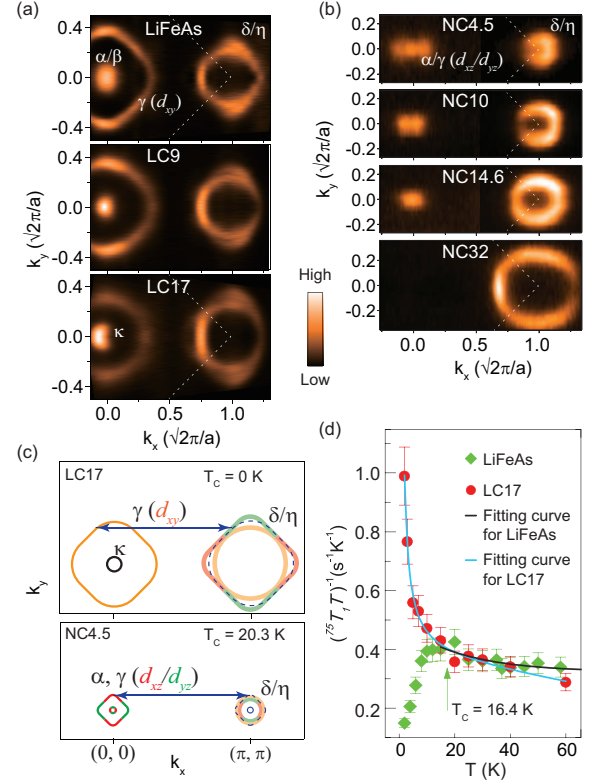


FIG. 2: (a) Doping evolution of the photoemission intensity map in $\text{LiFe}_{1-x}\text{Co}_x\text{As}$ taken with 21.2 eV photons in mixed polarization. (b) Doping evolution of the photoemission intensity map in $\text{NaFe}_{1-x}\text{Co}_x\text{As}$ taken with 100 eV photons in linear polarization. (c) Illustration of the FS nesting condition in LC17 and NC4.5 . (d) The spin-lattice relaxation rate $1/T_1 T$ of LiFeAs and LC17 under a field of 8 T and 11.5 T respectively, applied along the crystal *ab* plane. The solid line is a fit by a Curie-Weiss term $1/T_1 T = A + B/(T - \Theta)$ with $\Theta = -20 \pm 5$ K for LiFeAs and $\Theta = -0.7 \pm 5$ K for LC17 . See ref. [20] for the NMR experimental details.

Replacing Fe with Co introduces electrons into the system. As shown in Figs. 2(a) and 2(b), the hole pockets shrink with Co doping while the electron pockets are enlarged. According to the spin-fluctuation-mediated pairing scenario [15, 16], similar sizes of hole and electron pockets will give better nesting and thus enhance the scattering from zone center to zone corner, which will benefit the superconducting pairing. For $\text{LiFe}_{1-x}\text{Co}_x\text{As}$, the nesting condition for the d_{xy} hole pocket is improved with Co doping. However, the T_c is suppressed. We could even achieve a nearly perfect nesting between the d_{xy} hole pocket and the electron pockets in LC17 , but it is not superconducting at all [the upper panel of Fig. 2(c)]. On the contrary, in NC4.5 the d_{xz}/d_{yz} hole pockets are well nested with the electron pockets, and its T_c is the highest one in this series [the lower panel of Fig. 2(c)]. With further electron doping, the nesting worsens and T_c decreases [Fig. 2(b)]. The comparison between $\text{LiFe}_{1-x}\text{Co}_x\text{As}$ and $\text{NaFe}_{1-x}\text{Co}_x\text{As}$ indicates that the FS nesting does enhance superconductivity, but only when it is between d_{xz}/d_{yz} FSs. This is consistent with the larger superconducting gaps on the d_{xz}/d_{yz} FSs here

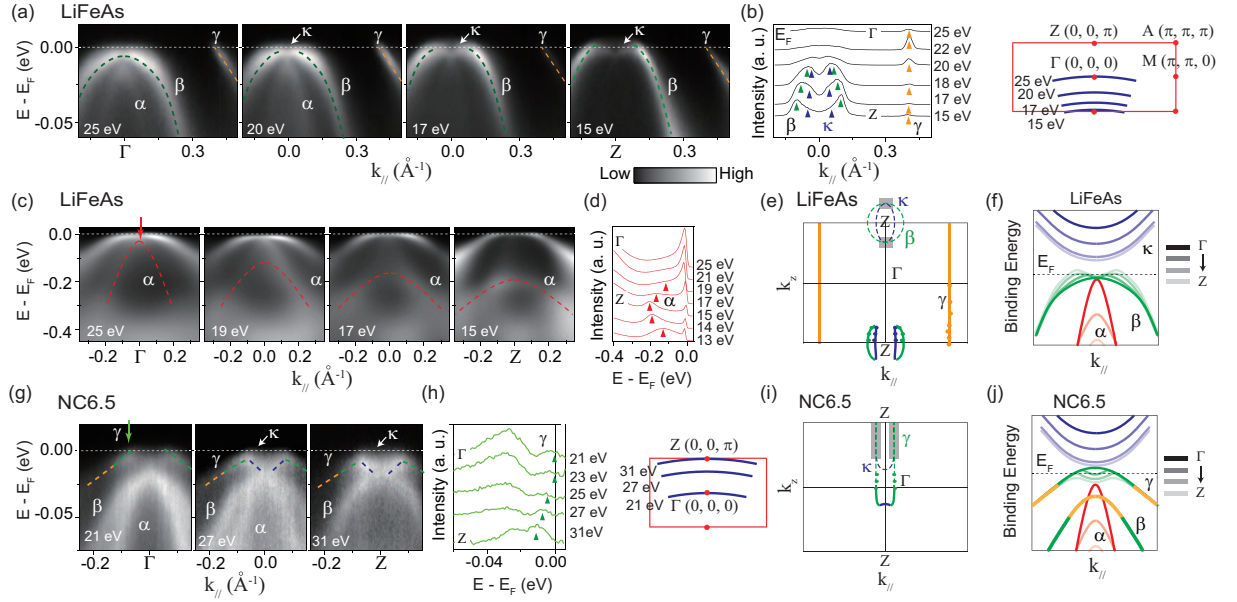


FIG. 3: Panels (a) - (f) are the k_z dependent data for LiFeAs. (a) and (b), Photon energy dependence of the photoemission spectra and the momentum distribution curves (MDCs) at E_F taken along $(0, 0) - (\pi, \pi)$ direction. (c) and (d), Photon energy dependence of the photoemission spectra with a larger energy scale and the energy distribution curves (EDCs) at $k_{\parallel} = 0 \text{ \AA}^{-1}$ taken along $(0, 0) - (\pi, \pi)$ direction. (e) Illustration of the FS cross-section in $Z - \Gamma - M - A$ plane. The upper half of panel (e) shows the hybridization between β and κ pockets. Gap opens in the gray marked sections. (f) is a Cartoon showing how the bands evolve from Γ (represented by darker color) to Z (represented by lighter color). (g) - (j) are the same as (a), and (d) - (f), respectively, but for NC6.5. The EDCs in (h) are taken at the Fermi crossings as indicated by the green arrow in panel (g).

shown in Figs. 4(d) and 4(h), and for $\text{Ba}_{0.6}\text{K}_{0.4}\text{Fe}_2\text{As}_2$ as well [10, 19]. Moreover, we compare the strength of spin fluctuations in LiFeAs and LC17 measured by the nuclear magnetic resonance (NMR). The fitting parameter Θ (Curie-Weiss temperature) of LC17 is much larger than that of LiFeAs, indicating stronger low-energy spin fluctuations in LC17 [Fig. 2(d)]. However, it is important to note that T_C is not enhanced by such an enhancement of the low-energy spin fluctuations due to the nesting of the d_{xy} FSs.

To further study the Fermiology in 3D momentum space, Fig. 3(a) shows the k_z evolutions of the bands around the zone center in LiFeAs, obtained by changing the incident photon energy (top right inset of Fig. 3). From Γ to Z , the band top of β gradually shifts toward E_F , and finally crosses E_F around Z . Meanwhile, an electron-like band named κ emerges at the photon energy of $\sim 20 \text{ eV}$, and hybridizes with β , exhibiting a “M”-like feature near E_F . The Fermi crossings of β , κ , and γ could be traced clearly from the MDCs near E_F [Fig. 3(b)]. The observation of κ electron pocket is notable. According to band calculations, there is a fast dispersing electron band along the k_z direction whose band bottom is far above E_F at Γ , but shifts downward quickly when approaching Z [21]. It has been proposed that when the bottom of this band touches α/β , the top of α will be pushed downwards away from E_F [22]. Consistently, in Figs. 3(c) and 3(d), the top of α shifts downwards quickly from Γ to Z . Such a strong k_z dispersion of α and the appearance of κ produce a distinctive 3D Fermiology for the d_{xz}/d_{yz} hole pocket. As shown in Fig. 3(e), β forms

an ellipsoidal hole FS along the k_z direction, while the κ electron pocket appears around Z and hybridizes with the β hole pocket. As a result, the energy gaps open on the crossings of the two FS sheets, forming two banana-like shaped FS cross-sections. The k_z evolution of the band structure of LiFeAs is illustrated in Fig. 3(f). Note that, the finite k_z resolution of ARPES will smear out the bands with strong k_z dispersions. As shown in Fig. 3(c), the band dispersion of α at Γ still contributes finite spectra weight at 19 eV and 17 eV. This is perhaps why such a strong k_z dispersion of this band was missed in previous ARPES experiments.

For NC6.5, as shown in Fig. 3(g), the κ electron pocket emerges at 27 eV and opens a hybridization gap with the γ band [Fig. 3(h)], which resembles that in LiFeAs. However, the 3D FS topology is very different in NC6.5. As shown in Figs. 3(i) and 3(j), the γ band contributes a cylindrical hole FS from Γ to Z . When the κ band appears around Z , κ and γ cross and opens a hybridization gap, and consequently the FS evolves into a drum-like hole pocket surrounding Γ .

Now we examine how these d_{xz}/d_{yz} -based 3D FSs evolve with doping in $\text{LiFe}_{1-x}\text{Co}_x\text{As}$ and $\text{NaFe}_{1-x}\text{Co}_x\text{As}$. Figure 4(a) demonstrates the doping evolution of the low lying electronic structures in $\text{LiFe}_{1-x}\text{Co}_x\text{As}$ measured by a 7 eV Laser. With Co doping, all the bands shift downwards, and the κ electron pocket could be clearly observed in LC9 and LC12. Note that, the β band with a strong k_z dispersion is broadened or even split at E_F due to the finite k_z resolution or final state effect. This suggests that the k_z broadening effect should also be care-

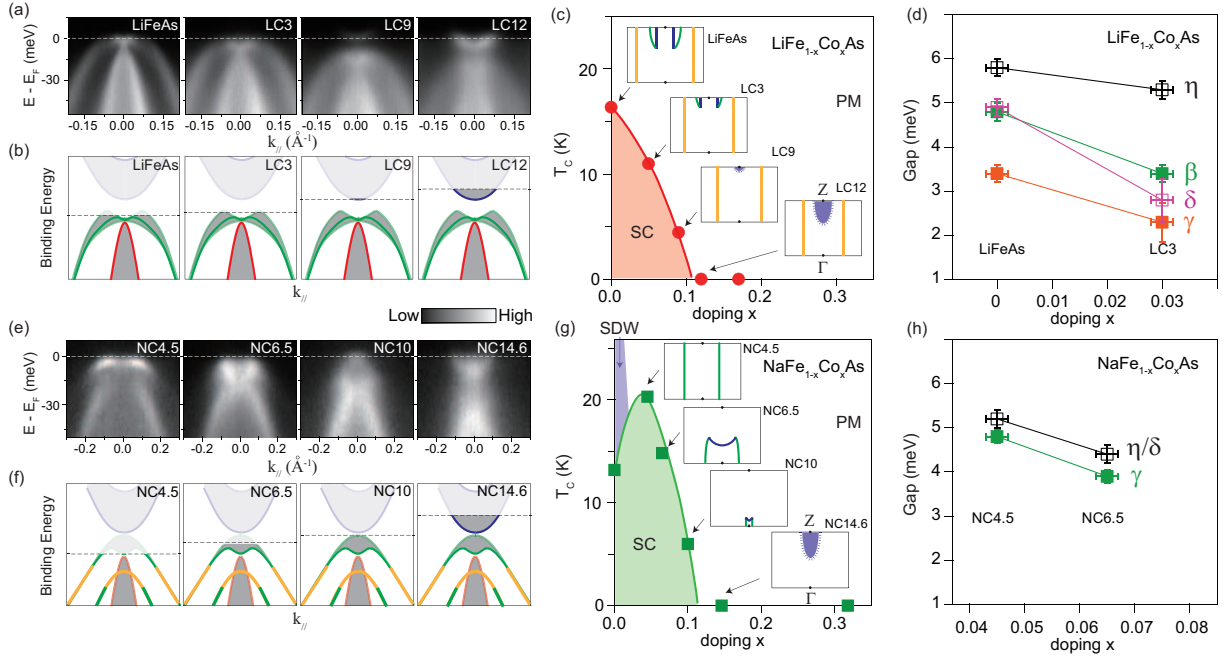


FIG. 4: (a) Doping dependence of the electronic structure around the zone center in $\text{LiFe}_{1-x}\text{Co}_x\text{As}$, taken with a 7eV laser. (b) is illustrations of the bands in (a). (c) The phase diagram and corresponding FS topology for $\text{LiFe}_{1-x}\text{Co}_x\text{As}$ near zone center. (d) The doping dependence of superconducting gap in $\text{LiFe}_{1-x}\text{Co}_x\text{As}$. The gap sizes are determined by symmetrized EDC's taken on different FSs (See supplementary information). (e) - (h) are the same as (a) - (d), but for $\text{NaFe}_{1-x}\text{Co}_x\text{As}$. The spectra in panel (e) are taken with 31 eV photons. In panels (c) and (g), the solid lines represent hole FSs, while dashed ones with blue area inside represent electron FSs.

fully considered even in laser-based ARPES experiments. We thus compare the spectra with the experimentally-determined band structure integrated from Γ to Z in Fig. 4(b). Figure 4(c) illustrates the corresponding 3D FS topology for different doping levels. With Co doping, the banana-like hole pockets sink away from E_F and the κ electron pocket emerges around Z in LC12 sample. Similar phenomena could be also observed in $\text{NaFe}_{1-x}\text{Co}_x\text{As}$ [Figs. 4(e) - 4(g)]. The d_{xz}/d_{yz} FS is a cylinder in NC4.5 and shrinks with Co doping. In NC14.6, κ electron pocket emerges. The FS evolution of $\text{LiFe}_{1-x}\text{Co}_x\text{As}$ and $\text{NaFe}_{1-x}\text{Co}_x\text{As}$ clearly shows that the d_{xz}/d_{yz} FS undergoes a Lifshitz transition. Although the Fermiology is dramatically different for $\text{LiFe}_{1-x}\text{Co}_x\text{As}$ and $\text{NaFe}_{1-x}\text{Co}_x\text{As}$, we found in both cases that the superconductivity disappears just quickly after the disappearance of the d_{xz}/d_{yz} hole FSs [Figs. 4(c) and 4(g)]. Our results thus suggest the importance of the presence of central d_{xz}/d_{yz} hole FSs for the superconductivity in Fe-HTS's. Such an orbital selective correlation between Lifshitz transition and superconductivity is resolved for the first time. In addition, we note that LC9 is still superconducting below 5K, while the small κ FS has appeared at E_F [Fig. 4(c)]. It is likely due to some residual superconducting pairing amplitude contributed by the rest of the FSs, after the d_{xz}/d_{yz} hole FSs sink below E_F . When the κ FS grows bigger at higher doping, it does not help the superconductivity. In the inter-pocket pairing scenario, it is known that the pairing strength would be weak if the Fermi velocities at the zone corner and zone center hold the same sign. That is, superconductivity would

not be enhanced when both are electron FSs around the zone center and corner, as is the case for our data. Alternatively, the suppression of superconductivity could be viewed through the decreasing superconducting gap [Figs. 4(d), 4(h), and supplementary information], which is roughly proportional to T_C .

The orbital selective correlation between superconductivity and the electronic structure is also manifested in the impurity scattering effects. As shown in Fig. 5(a), with Co doping, the d_{xy} -based γ band becomes significantly weaker and broader. Figs. 5(b) - 5(e) plot the MDCs at E_F and 50 meV below the band top of the α/β bands, together with the full-width-half-maximum (FWHM) of various bands. The FWHM of γ increases remarkably with Co doping comparing to all the other bands. On the other hand, because the band top of α/β shifts away from E_F , the increasing binding energy causes the slight increase of FWHMs with doping for the α and β bands in Fig. 5(e). Therefore, the FWHMs of η , α and β are essentially insensitive to the Co dopants. Similar phenomena is also observed in $\text{NaFe}_{1-x}\text{Co}_x\text{As}$ [Figs. 5(f) and 5(g)]. Such orbital-selective scattering effects of the Co dopants need further theoretical understandings. However, it might explain the robust superconductivity against heavy doping in Fe-HTS's, since most bands with d_{xz} and d_{yz} orbitals are basically unaffected by the scattering of dopants. Furthermore, a recent STM study of $\text{NaFe}_{1-x}\text{Co}_x\text{As}$ shows that the low energy electronic state is somehow insensitive to the Co-dopant [23]. Our data provide an explanation: the tunnelling matrix element might be weak for the in-plane d_{xy} orbital that is most sensi-

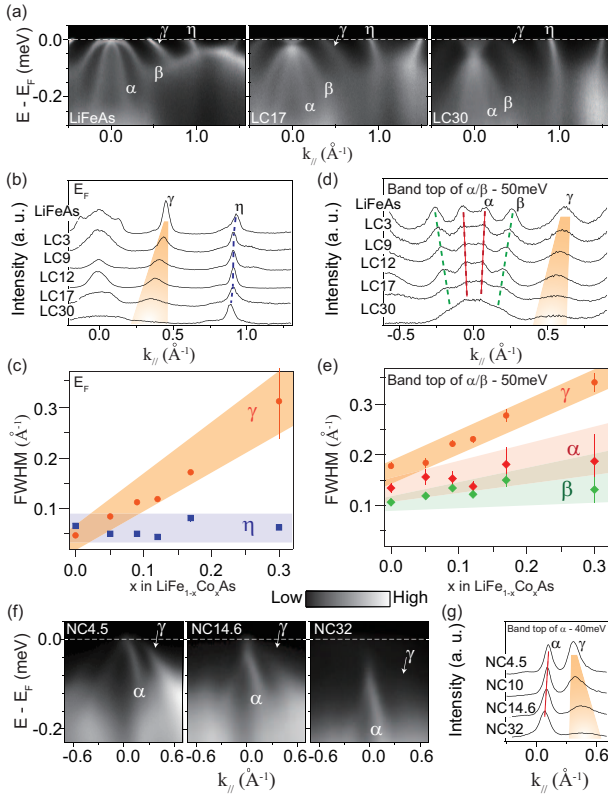


FIG. 5: (a) Doping dependence of the photoemission intensities of $\text{LiFe}_{1-x}\text{Co}_x\text{As}$. (b) The doping dependence of the MDCs at E_F . (c) is the corresponding FWHMs of γ and η in (b). (d) MDCs at 50 meV below the band top of α/β as a function of doping, since α and β do not cross E_F . (e) is the corresponding FWHMs of α , β and γ in (d). (f) Doping dependence of the photoemission intensities in $\text{NaFe}_{1-x}\text{Co}_x\text{As}$. (g) Doping dependence of the MDCs at 40 meV below the band top of α in $\text{NaFe}_{1-x}\text{Co}_x\text{As}$.

tive to the impurity scattering.

The correlations that we found here for iron pnictides between the superconductivity and the hole FSs around the zone center do not apply to $\text{K}_x\text{Fe}_{2-y}\text{Se}_2$ and the single FeSe layer on SrTiO_3 substrate [24–26]. They both have high T_C 's but no hole pockets. Scattering between the electron pockets around the zone corner was suggested to be important for the superconductivity in these iron selenides [27]. Interestingly, the FS of NC32 is almost the same as that of $\text{K}_x\text{Fe}_{2-y}\text{Se}_2$ [Fig. 2(b)], but NC32 is not superconducting. Our results indicate that the superconducting mechanism of these iron selenides are remarkably different from that of iron pnictides. Other factors may come into play, for example, the lattice constants of these iron selenides are much larger than those of iron pnictides [25].

To summarize, our results substantiate the pivotal role of the d_{xz}/d_{yz} orbitals in the superconductivity of $\text{AFe}_{1-x}\text{Co}_x\text{As}$ ($\text{A}=\text{Li}, \text{Na}$), and establish the orbital selective correlation between the superconductivity and the Fermiology. Although the Fermiology is dramatically different in these two series, we demonstrate that the superconducting T_C is maximized

only by the perfect nesting between d_{xz}/d_{yz} -originated FSs, while the superconductivity diminishes quickly after the central d_{xz}/d_{yz} hole FSs disappear with electron doping. Moreover, we found that the d_{xz}/d_{yz} orbitals are rather insensitive to impurity scattering. Our results thus could be used to simplify theories for the superconductivity in iron pnictides [28, 29], and help to design new materials to enhance T_C based on the Fermiology. It also clarifies many previous contradicting statements on the correlations.

We gratefully acknowledge the experimental support by Dr. D. H. Lu, Dr. R. G. Moore at SSRL, Dr. M. Arita at HiSOR and Dr. M. Shi at SLS. This work is supported in part by the National Science Foundation of China, and National Basic Research Program of China (973 Program) under the grant Nos. 2012CB921400, 2011CBA00112. SSRL is operated by the US DOE, Office of BES, Divisions of Chemical Sciences and Material Sciences.

* Electronic address: bpxie@fudan.edu.cn

† Electronic address: dleng@fudan.edu.cn

- [1] Y. Tokura and N. Nagaosa, et al., *Science* **288**, 462 (2000).
- [2] Y. Tokura, Ed., Gordon and Breach Science, New York, (2000), and references therein.
- [3] S. Kasahara, et al., *Nature* **486**, 382-385 (2012).
- [4] I. R. Fisher, L. Degiorgi, and Z. X. Shen, *Rep. Prog. Phys.* **74**(12), 124506 (2011).
- [5] Ming Yi, et al., *Proceedings of the National Academy of Sciences* **108** (17), 6878-6883 (2011).
- [6] Y. Zhang, et al., *Phys. Rev. Lett.* **105** (11), 117003 (2010).
- [7] Y. Zhang, et al., *Nature Phys.* **8** (5), 371-375 (2012).
- [8] M. Daghofer, A. Nicholson, A. Moreo and E. Dagotto, *Phys. Rev. B* **81** (1), 014511 (2010).
- [9] S. Graser, et al., *New J. Phys.* **11**, 025016 (2009).
- [10] H. Ding, et al., *EPL (Europhysics Letters)* **83** (4), 47001 (2008).
- [11] K. Terashima, et al., *Proceedings of the National Academy of Sciences of the USA (PNAS)* **106**, 7330-7333 (2009).
- [12] F. L. Ning, et al., *Phys. Rev. Lett.* **104** (3), 037001 (2010).
- [13] Chang Liu, et al., *Phys. Rev. B* **84** (2), 020509 (2011).
- [14] S. V. Borisenko, et al., *Phys. Rev. Lett.* **105**, 067002 (2010).
- [15] K. Kuroki, et al., *Phys. Rev. Lett.* **101** (8), 087004 (2008).
- [16] I. I. Mazin, D. J. Singh, M. D. Johannes, and M. H. Du, *Phys. Rev. Lett.* **101** (5), 057003 (2008).
- [17] M. Yi, et al., *New J. Phys.* **14**, 073019 (2012).
- [18] Y. Zhang, et al., *Phys. Rev. B* **85** (8), 085121 (2012).
- [19] D. V. Evtushinsky et al., arXiv:1204.2432 (unpublished).
- [20] L. Ma, J. Zhang, G. F. Chen and W. Yu, *Phys. Rev. B* **82** (18), 180501 (2010).
- [21] D. J. Singh, *Phys. Rev. B* **78**, 094511 (2008).
- [22] Hidetomo Usui, et al., arXiv:1204.1717 (unpublished).
- [23] H. Yang et al., *Phys. Rev. B* **86** (21), 214512 (2012).
- [24] Y. Zhang et al., *Nature Mater.* **10** (4), 273-277 (2011).
- [25] S. Y. Tan et al., arXiv, 1301.2748 (unpublished).
- [26] Shaolong He et al., arXiv, 1207.6823 (unpublished).
- [27] T. A. Maier, P. J. Hirschfeld and D. J. Scalapino, *Phys. Rev. B* **86** (9), 094514 (2012).
- [28] K. Seo, B. A. Bernevig and J. Hu, *Phys. Rev. Lett.* **101** (20), 206404 (2008).
- [29] J. Hu and N. Hao, *Physical Review X* **2** (2), 021009 (2012).